The GIMP Retinex Filter Applied to the Fabric Fault Detection

Journal Title
Journal **XX** (XXXX) XXXXXX https://doi.org/XXXX/XXXX

Role of the solvent in the activation of Li_2S as cathode material: A DFT study

Juan J. Velasco*, Patricio Vélez, Martin E. Zoloff Michoff, Arnaldo Visintín, Daniele Versaci, Silvia Bodoardo, Guillermina L. Luque, Ezequiel P. M. Leiva*

INFIQC, Departamento de Química Teórica y Computacional, Facultad de Ciencias Químicas, Universidad Nacional de Córdoba, CONICET, Ciudad Universitaria, X5000 Córdoba, Argentina
DISAT, Department of Applied Science and Technology, Electrochemistry Group, Politecnico di Torino, C.so Duca degli Abruzzi 24, 10129 Torino, Italy

E-mail: ezequiel.leiva@unc.edu.ar

Received xxxxxx
Accepted for publication xxxxxx
Published xxxxxx

Abstract

Lithium−sulfur batteries are considered one of the possible next-generation energy-storage solutions, but to be commercially available many drawbacks have yet to be solved. One solution with great potentiality is the use of lithium sulfide as cathode material since it can be coupled to Li-free anodes, such as graphite, Si or Sn. Nevertheless, Li_2S, like sulfur, is electronically and ionically insulating, with a high activation potential for its initial oxidation step. To overcome this issue, different strategies have been explored, one of them being the use of catalytic surfaces. In the present article, we study using first principles calculations the effect of the dielectric constant of the solvent on the activation energy of the cleavage reaction of Li_2S on different catalytic surfaces. To the best of our knowledge, this is the first time that such a study is undertaken. We find that the effect of the solvent should be twofold: On one side, it should decrease the interaction between the Li_2S molecule and the surface. On the other side, since the species arising in the dissociation reaction are charged, the solvent should decrease the activation barrier for the dissociation of the Li_2S molecule, when compared with the reaction in vacuum. These theoretical findings arediscussed in connection with experimental results from the literature, where the behaviour of the Li-S cathode is studied in different solvents.

Keywords: Li_2S cathodes, solvent dielectric constant, metallic sulfides, catalytic surfaces

1. Introduction

Among the most promising post-Li-ion technologies, lithium-sulfur (Li-S) batteries have attracted a considerable deal of attention mainly due to their high theoretical specific capacity (1675 mAh g^{-1}) and the low cost of raw sulfur (<$150/ton). However, the implementation of Li-S batteries in daily life applications still presents several handicaps that must be overcome: The low conductivity of sulfur, Li_2S and Li_2S_2 species; the concomitant large volume expansion upon discharge; and the occurrence of soluble polysulfide species that migrate from one electrode to the other upon battery cycling leading to the so-called shuttle effect. The latter leads to the discharge of these species on the lithium metal anode, which rapidly leads to battery failure. Furthermore, the charge and discharge of the lithium metal anode have their own problems: formation of dendrites, dead lithium, just to mention a few, which are also being the subject of intensive research. Several reviews in the literature deal with these subjects in-depth, so we will not extend into these problems

here [2–7]. For the present work, it is of interest the emergence of the Li_2S cathode paradigm: this compound participates in a battery as the cathode material and can be efficiently coupled to Li-free anodes, such as graphite, Si or Sn, eliminating the use of Li metal as the anode. Thorough reviews [8–10] have been published on this topic, including one very recent by Ye *et al.* [11]. Although the Li_2S cathode presents several advantages, the main problem with this setup is the activation of Li_2S for its oxidation to sulfur: this reaction has extremely slow kinetics, with electrochemical activation barriers of the order of 3 V. Different strategies have been developed to tackle this problem, as discussed in [11]: Nanostructuring, amorphization, doping, electrolyte additives, redox mediators and the use of electrocatalysts. The latter approach is devoted to decreasing the activation energy barrier of the intermediate involved in the rate-determining step. In this respect, different approaches have been taken which will be discussed in the next paragraphs.

Wu et al. [12], have used nanostructured $Li_2S@LiTiO_2$ composite electrodes, exhibiting a strong bonding of the titanate with Li_2S and inducing a rapid conversion of long polysulfides to short ones. These authors have also shown employing DFT calculations, that long polysulfides strongly adsorb and dissociate on $LiTiO_2$ surfaces. They also found that solvent molecules should be easily displaced from the surface by polysulfides.

Yuan et al. [13] have found an efficient activation of Li_2S by different transition metal phosphines nanoparticles such as Ni_2P, Co_2P, and Fe_2P. DFT calculations by these authors demonstrated that Ni_2P, Co_2P, and Fe_2P present much higher adsorption energy towards Li_2S than pure or N-doped carbon. Furthermore, they found that the dissociation energies of Li_2S on these phosphine surfaces are considerably lower than that for pristine carbon or N-doped carbon, thus providing support to the improved catalytic activity found for the phosphines.

Liang et al. [14] have prepared a multi-layer Ti_3C_2/Li_2S cathode by ball-milling, finding a reduction of 0.6 V in the activation voltage barrier when compared with a graphene/Li_2S composite cathode.

Shin et al. [15] studied a Li_2S@graphene cathode with a ZnS coating, finding that it decreases the necessary activation potential needed for the oxidation of Li_2S to sulfur in comparison with the uncoated cathode. In this case, DFT calculations were used to analyse the interaction of ZnS with DOL and DME in comparison with graphene as a substrate.

Zhou et al. [16] have studied the catalytic oxidation of Li_2S on different metal sulfides, and with the aid of DFT calculations, they demonstrated that the energy barrier for Li_2S decomposition is associated with the binding between isolated Li ions and the sulfur in sulfides. More recent work by He et al. [17] has confirmed the important electrocatalytic behaviour of different transition polysulfides (CoS, NiS, MnS) decorating carbon sponges, with dramatic improvements in reducing the potential barrier for Li_2S activation.

All the previous work shows the importance of different catalysts for Li_2S, as well as the relevance of DFT calculations for their understanding. Turning to a related problem, a recent DFT work [18] has shown the importance of solvent in the bond cleavage reactions of polysulfide intermediates in bulk solution. These authors investigated the relationship between the donor numbers and the dielectric constants of the solvent system and the relative stability of different polysulfide intermediates.

The usual experimental approach to test catalysts for the Li_2S activation consists of performing several galvanostatic cycles of charge/discharge steps and monitoring the specific capacity as a function of the number of cycles. The experimental response of the system under these conditions is a very complex convolution of several factors affecting the performance. For example, the presence of dissolved polysulfides may itself act as a mediator improving the oxidation of Li_2S in the first cycle [19]. Since the solubility of the polysulfide is a function of the solvent, it is very difficult to assess the role of the later in the Li_2S activation. Thus, theoretical work may be useful to disentangle the different factors controlling the performance of the present cathode. The present work adds an important contribution in this direction as we consider the influence of the dielectric constant of the solvent on the cleavage reaction of Li_2S on different catalytic surfaces. To the best of our knowledge, this is the first time that such a study is undertaken.

2. Methods

2.1 Computational Details

Ab-initio calculations were performed to study energy decomposition barriers for Li_2S on different surfaces. From the density functional theory approach, calculations were carried out using the Quantum Espresso computer code. Generalized-gradient approximation (GGA) of the Perdew-Burke-Ernzerhof (PBE) [20] functional was used to describe exchange and correlation effects. Core electrons were

modelled by pseudopotentials in the projected-augmented wave method (PAW). Van der Waals interactions were considered through semiempirical Grimme's DFT-D2 [21] correction. All the calculations were performed taking into account spin polarization.

Metal sulfides surfaces were represented using a supercell with periodic boundary conditions, modeled by 3x3x1 slab for VS_2 and by 2x2x2 slab for MnS in the (001) plane. Graphene was modeled as a 6x4 repeated carbon shell unit. Convergence studies were done for setting up the relevant parameters for each system. The kinetic energy cutoff used for wave functions was 50 Ry, while for charge density and potential it was 400 Ry. Brillouin zone integration was approximated using the Monkhorst-Pack [22] scheme with 4×4×1 k-point sampling. A 20 Å vacuum space between slabs in the z-direction was enough to avoid artificial interaction effects due to the periodicity.

Climbing image nudged elastic band (CI-NEB) [23] method was used to study the decomposition barrier energy for Li_2S in two different situations: a) the isolated molecule and b) the molecule adsorbed on metal sulfides surfaces and pristine graphene. These types of surfaces were reported in the literature to have promising catalytic effects [16,17,24–27]. For this work, two transition metal sulfides were selected: VS_2, and MnS [16].

As has been mentioned above, we are interested in the solvent effects for the reaction $Li_2S \rightarrow LiS + Li^+ + e^-$. Some earlier reports in the literature have suggested the crucial role of solvents for this reaction in Li-S batteries [28–32], but to the best of our knowledge, there is no systematic work considering its effect on the present reaction. In our computer simulations, the solvent was introduced utilizing an embedding continuous model, as described in more detail below.

2.2 Solvent Model

The Environ library available for Quantum Espresso was implemented for solvent corrections [33,34]. The physical picture of the model could be seen as the addition of a continuum polarizable dielectric around the solute. The dielectric response to the charge distribution of the solute is fully characterized by its dielectric constant, ε. Energy and forces corrections were included in Ci-NEB calculations.

In the present article, we have considered a wide range of dielectric constant values of solvents. Among them, the most typical ones used in the field of Li-S batteries considered in this study were dimethylformamide (DMF, ε = 36.7), and dimethoxyethane (DME, ε = 7.2). The dielectric function was defined by the soft-sphere continuum solvation (SSCS) model [35] This interface model has been proved to be adequate for lithium, due to its low electronic density. Parabolic point counter charge correction was included for surface calculations to avoid artificial interactions between periodic images [36]. Finally, atomic radii were defined according to Bondi's work [37]. Solvation energy and Li-S bond distances for the optimized Li_2S molecule were reproduced according to literature with these settings [28].

3. Results and Discussion

In the following subsections, the main results of this work are presented and discussed, as follows: Firstly, the effect of the solvent on the Li_2S adsorption on the different surfaces is considered. Thereafter Li_2S decomposition, isolated and adsorbed on graphene and the metal sulfide surfaces, is fully discussed both in vacuum and in the presence of a solvent represented by the interaction with a dielectric.

3.1 Solvent effect on the Li_2S adsorption

In the first stage, a conjugate-gradient optimization was carried out for the Li_2S molecule adsorbed on each of the surfaces studied. Lattice parameters reported by the literature were reproduced in all the cases [38–40]. The corresponding binding energies (E_b) were thus obtained according to eq. (1), where E_T is the energy of the entire system (ie. surface + Li_2S) in the relaxed configuration, E_{surf} the energy of the corresponding clean surface, and E_{Li_2S} the energy of the isolated molecule.

$$E_b = E_T - E_{surf} - E_{Li_2S} \qquad \text{eq.(1)}$$

According to this equation, more negatives values for E_b are related to a stronger interaction between the molecule and the surface. Table 1 summarizes the values obtained for E_b in the absence of solvent effects (ie. at ε = 1). These results show that the binding strength of Li_2S is notably much higher for the polar metal sulfides than for the apolar carbonaceous surface, and follows the order Graphene << VS_2 < MnS.

We note in passing, that it has often been argued that more negative values for E_b are linked to stronger electrocatalytic effects [41]. This assessment is reasonable in terms of bond-order conservation, ie. the formation of new bonds with the surface should weaken the internal bonds of a molecule, making it more prone to react.

Surface	E_b / eV
Graphene	-1.33
VS_2	-3.15
MnS	-3.59

Table 1: Binding energies (E_b), as defined in eq. (1), for the adsorption of a Li_2S molecule on the surface indicated in the first column in vacuum (ε = 1).

To assess the effect of solvent on the adsorption/desorption equilibrium, systematic ab initio calculations were performed for each Li_2S/surface combination and different values of dielectric constants in the range of 1 - 80. As shown in Fig. 1, E_b becomes rapidly less negative as the dielectric constant increases, indicating a weakening of the molecule - surface interaction.

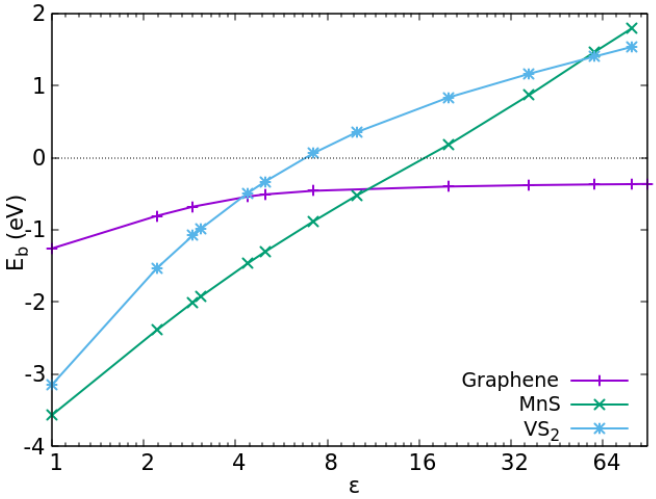

Figure 1: Binding energy of a Li_2S molecule on different surfaces immersed in a dielectric as a function of the logarithm of the dielectric constant.

Notably, in the case of graphene, E_b rapidly reaches a limiting value of ca. -0.5 eV at $\varepsilon > 4$. On the other hand, for the metal sulfides, the adsorption energy becomes eventually positive, indicating that at a given value of ε the molecule desorption is thermodynamically favourable and will therefore no longer remain adsorbed. These limiting values are $\varepsilon = 6.8$, and $\varepsilon = 16.8$, for VS_2 and MnS, respectively.

The different behaviour of graphene and the sulfides can be understood in terms of the interaction of the different surfaces with the dielectric medium. In the case of graphene, the surface is expected to be relatively smooth from the viewpoint of the charge density, while in the case of the metal sulfides, their heterogeneous chemical nature is expected to yield a stronger interaction with the solvent. To get a quantitative descriptor of the heterogeneity of the surface charge, we have calculated the sum of the squares of the Bader atomic charges of the surface atoms, termed as S_{Bader}, eq. (2), where Q_i is the Bader charge on atom i and A is the area of the slab.

$$S_{Bader} = \frac{\sum_i Q_i^2}{A} \qquad \text{eq. 2}$$

The S_{Bader} values obtained for the systems studied in this work are summarized in Table 2 for the two values of ε presently studied, namely 1 and 10.

System	S_{Bader} (ε=1)	S_{Bader} (ε=10)
Graphene	0.001	0.001
VS_2	0.095	0.095
MnS	0.439	0.439

Table 2: Sum of the squares of the Bader atomic charges of the surface atoms, S_{Bader}, as defined in eq. (2), for the different systems considered here and for two values of the dielectric constant presently studied.

From this table, it can be seen that the two metal sulfide systems considered present a considerably larger value of S_{Bader} than graphene, indicating that the solvent polarization is already very important even before the adsorption of the Li_2S molecule.

Interestingly, the polar nature of the metal - sulfur bonds has a two-fold consequence for the Li_2S adsorption on metal sulfides: on one hand, it provides a stronger interaction when compared with an apolar surface such as graphene, which should enhance the catalytic effect towards Li_2S oxidation; and on the other, this interaction becomes rapidly less favoured from a thermodynamic point of view in environments with $\varepsilon > 6.8$ - 16.8 depending on the nature of the transition metal.

3.2 Li_2S decomposition in solvent embedding cavity

The decomposition of an isolated molecule, ie. in absence of a surface, was studied as a reference reaction. The decomposition process was considered for a single Li_2S molecule, into LiS and a Li atom. The overall process consists of breaking one of the Li-S bonds. The energy profile obtained from the CI-NEB in vacuum ($\varepsilon = 1$), is shown in Fig. 2 as the black curve. The energy profiles for breaking the Li-S bond were calculated for increasing values of ε in the range 2.21 - 80, keeping the configurations obtained for the reaction pathway in vacuum, and are also illustrated in Fig. 2.

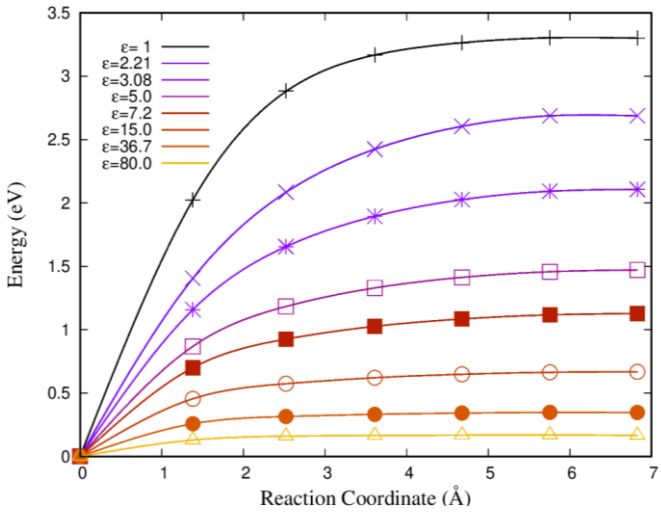

Figure 2. Energy profiles for the decomposition reaction of a single isolated (in the absence of a surface support) Li_2S molecule as a function of the reaction coordinate for different values of ε in the range 1 - 80.

The decomposition energy barrier for lithium sulfide in vacuum is 3.28 eV (see Fig. 2). As the dielectric constant of the continuum solvents increases, the energies profiles change significantly. The barrier drops dramatically, and at a value of ε = 5 the energy barrier is reduced to less than one half of the corresponding value in vacuum. Among the specific ε values chosen for the calculations, we consider the cases of some typical organic solvent used in Li-S battery studies. The obtained energy barriers were 1.13 eV for DME (ε = 7.2) and 0.35 eV for DMF (ε = 36.7). This important dependence of the energy barrier on the solvent resembles the analysis of the stability of Li-polysulfides in different solvents done by Sun *et al.*[42]. These authors argued that the electrostatic interaction energy, as expressed by the Born equation, is proportional to 1/ε and accounts for the major portion (> 80%) in the solvation energetics of lithium salts and other ionic compounds. In this way, in the lower domain of the dielectric constant, these authors noticed that a small change in ε causes a considerable increase in the solubility of Li-polysulfides. Our results for the decomposition of Li_2S follow a similar trend.

3.3 Li_2S decomposition on a graphene surface

The first system with a surface involves graphene. The trajectory of the Li atom being separated from the molecule is shown in Fig. 3. In this case, the final position of the Li atom, after the breakage of the Li-S bond, corresponds to its adsorption on the centre of a hexagon of the graphene honeycomb lattice.

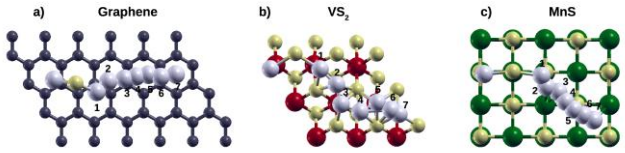

Figure 3: Trajectories of the Li atom being separated from the Li_2S molecule on a) graphene, b) VS_2 and c) MnS surfaces. The numbers on the graphs indicate the configuration of the lithium atom corresponding to the image in the reaction coordinate of the NEB path. C atoms are black, S atoms are yellow, V atoms are red, Mn atoms are green, and Li atoms are light blue.

The energy profiles *vs.* the reaction coordinate for Li_2S decomposition on the graphene surface for different values of the environment dielectric constant are shown in Fig. 4. The curve for ε = 1 closely resembles the one obtained by Zhou *et al.* [43], with a relatively high energy barrier of ca. 2 eV, which is, nonetheless, considerably smaller than that obtained for the molecule dissociation in vacuum (Fig. 2). While the energy of the last image for ε = 1 is 1.6 eV, the hump close to the end of the curve coincides with the configuration where the Li atom overcomes a bridge site between two C atoms (NEB image #6 in figure 4a).

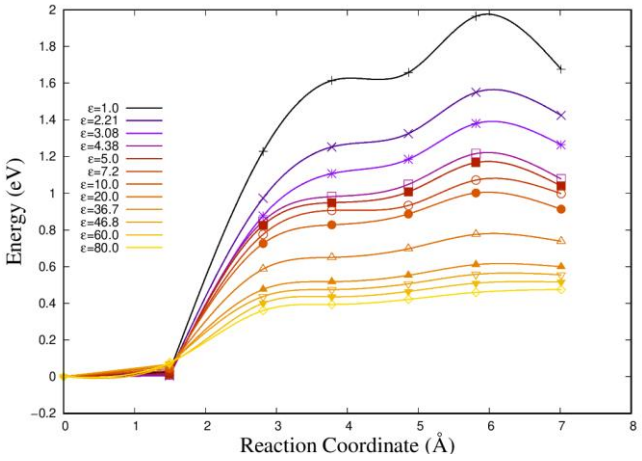

Figure 4: Decomposition energy profile as a function of the reaction coordinate for a Li_2S molecule adsorbed on graphene in contact with different solvents, characterized by their dielectric constant, ε.

This result shows that although there is rather weak interaction energy between Li_2S and the apolar graphene surface (see Table 1), the latter already presents some catalytic effect, reducing the energy barrier for the decomposition reaction by ca. 30% in vacuum. As in the case of the isolated Li_2S molecule, the energy barrier for the decomposition reaction on graphene is highly sensitive to the dielectric constant of the environment, displaying an

important decrease with increasing ε. The energy barrier decreases by ca. 2-fold at ε = 5.

3.4 Li_2S decomposition on Metal sulphide surfaces

As has already been mentioned above, metal sulphide surfaces have been shown to favour catalytic effects. The systems selected for this work correspond to those more promising in theoretical and experimental studies.

The first metal sulphide surface analysed was VS_2, which should exhibit the strongest catalytic activity, according to previous DFT work [16]. The decomposition energy profile for Li_2S on VS_2 is shown in Fig. 5. In vacuum (ε = 1), the energy profile fits previous DFT results [16]. The energy difference between the initial and final states is 0.42 eV. Along the decomposition pathway, the maximum value climbs up to 0.62 eV and corresponds to the lithium atom sitting on top of a S atom of the VS_2 surface (NEB image #6 in figure 3b). As can already be accounted for, the necessary energy to decompose Li_2S on this surface is approximately three times smaller than the one needed on a graphene surface, showing the catalytic effect of this metallic sulfide surface.

For an increasing value of the dielectric constant of the solvent, the energy barrier decreases steeply, up to a value of ca. 0.40 eV for ε values where the Li_2S molecule remains adsorbed on the surface (ε = 6.8, see Fig. 1).

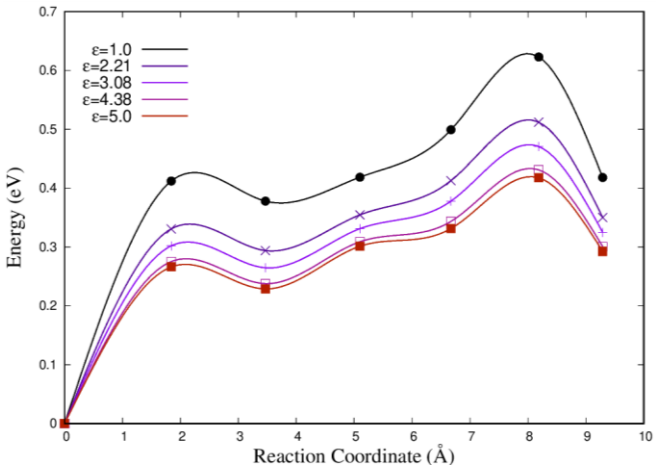

Figure 5: Decomposition energy profile as a function of the reaction coordinate for a Li_2S molecule adsorbed on VS_2 in contact with different solvents, characterized by their dielectric constant ε.

In the case of MnS, Li2S decomposition in vacuum presents activation energy of 1.2 eV that decays with the increasing value of the dielectric constant as can be seen in Figure 6. For values ε ≤ 3.08, the maximum along the reaction pathway corresponds to the lithium atom on top of a Mn atom of the metal sulfide structure. For larger values of ε, the maximum in the energy profile shifts to a position in which the lithium atom sits in the proximity of a Mn atom. Even though, in this case, the maximum value of the energy profile is smaller than the ones observed for graphene (even in the presence of solvent at the same value of dielectric constant); the energy barriers for MnS are larger than the ones found for the more catalytic surface V_2S. Here it is important to notice that although Li_2S presents larger binding energy on MnS in comparison with V_2S, for all the values of the dielectric constant considered, the catalytic effect is higher for the latter. Although it could be expected that the S-Li bond could be weaker when adsorbed on MnS, the morphology of the metal sulfide surfaces is quite different, suggesting that interaction of the final broken fragments might also be of different magnitude. The energy difference between the final and initial states for the decomposition pathways lies in the range of 0.60 - 0.80 eV for MnS, whereas for VS_2 is ca. 0.25 - 0.40, which has a direct impact on the corresponding energy barriers.

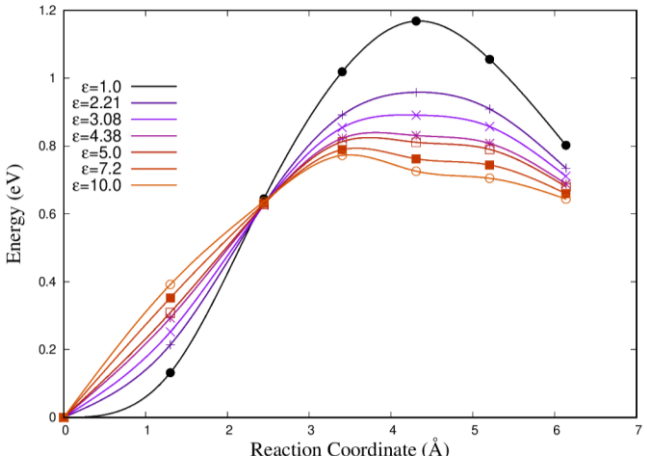

Figure 6: Decomposition energy barrier as a function of the reaction coordinate for a Li_2S molecule adsorbed on MnS in contact with different solvents, represented by their dielectric constant.

Figure 7 shows a plot of the activation energies (E_a) *vs*. ε for the decomposition reaction of Li_2S isolated and supported on the different surfaces considered in this work. In the case of the isolated molecule, it can be readily seen that the relationship between E_a and ε follows a power law in a wide range of ε, with an exponent close to -0.75, as obtained from the linear fit to selected data points, for the isolated case. A slope close to -1 would be expected in a naive electrostatic solvation approach, where the charge on the atoms remains constant, independent from the polarization of the environment. The observed decrease in slope denotes that the effective charges on the atoms taking part in the process tend to increase with increasing ε. This type of analysis provides

a meaningful comparison of the solvent effects for different situations. As it can be observed, the steepest slope is found for decomposition of the isolated Li_2S (orange line in Fig. 7), whereas for the different surfaces, the change of activation barrier with the dielectric constant of the solvent is less dramatic, as evidenced by the smaller values of the slopes, and it is quite similar among them. This can be understood in terms of the atomic charge on the lithium atom that breaks apart upon decomposition of Li_2S. As it can be gathered from Table 3, when the reaction takes place in the absence of surface support (isolated molecule), the charge on this Li atom is initially +0.3 in vacuum, and then when the solvent is considered it increases to a value that is close to +1. For the reaction taking place on surface support, the charge of the aforementioned lithium atom takes rather large values, in the range of +0.6 - 0.8, already in the absence of solvent. The inclusion of the solvent produces a rather mild increment to these values, thus explaining the less pronounced solvent effect for the metal sulfide surfaces and grapheme, as compared with the situation in the absence of such catalytic supports.

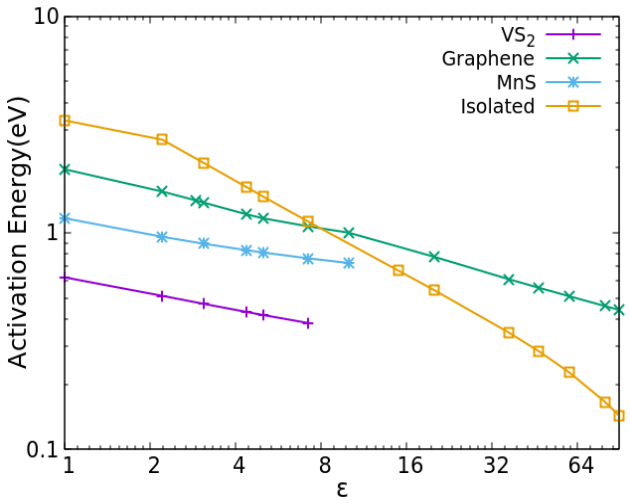

Figure 7: Activation energy for breaking the Li-S bond of the Li_2S molecule in the absence of a surface and on graphene, VS_2 and MnS surfaces, with different values of dielectric constant.

	ε= 1.0	ε = 10.0
Isolated	0.331	0.998
Graphene	0.638	0.674
MnS	0.778	0.791
VS_2	0.756	0.775

Table 3: Bader charge on the lithium atom in the final state of the scission of the Li-S bond of the Li_2S molecule at two values of dielectric constant both in absence of a surface and on the different surfaces considered.

3.5 Comparison with experimental results

Although the lithium sulphur battery has been the subject of extensive research, it is difficult to find experimental data that allow direct comparison with the present calculations. On one side, there are not many articles where the performance of the cathode is systematically studied in a variety of solvents, especially concerning the activation of Li_2S. On the other side, the behaviour of the battery is the emergent of several reaction steps that make it difficult to assess the role of Li_2S activation as considered here. In this respect, we hope that since we are addressing one of these steps, the present information may help to get indirect information on the others. Sun et al [42] have measured discharging/charging voltage profiles performing rate tests of Li−S cells with electrolytes of different compositions: DME:DOL = 50:50, DME:DOL:MTBE = 25:25:50, DME:DOL:DIPE = 25:25:50 and DME:DOL:MTBE = 12.5:12.5:75. We give in Table 4 the compositions of the different systems, and the average dielectric constants, calculated by weighting the εs of the pure solvents, and the oxidation potential for a c/2 charging rate. The latter was taken from the maximum observed in the discharge curve. Even though there is some indication for an increase in the oxidation potential as expected from the present calculations, the differences are very small and the dielectric constant range analysed is too restricted to draw enlightening conclusions.

Solvent	ε	Oxidation potential /V
DME:DOL = 50:50	7.25	2.40
DME:DOL:MTBE = 25:25:50	5.82	2.46
DME:DOL:DIPE = 25:25:50	5.57	2.49
DME:DOL:MTBE = 12.5:12.5:75.	4.88	2.44

Table 4: Solvent mixture, average dielectric constant and oxidation potential observed at the potential peak for galvanostatic c/2 charging using a S/ketjenblack mixture as cathode. Data taken from reference [42]. The solvents where 1,2-dimethoxyethane (DME, ε=7.20), 1,3 -dioxolane(DOL, ε =7.30), diisopropyl ether (DIPE, ε =3.88), Methyl, tert-butyl ether (MTBE, ε =4.38). The average dielectric constant $\underline{\epsilon}$ reported was calculated by straightforward weighing of the individual ε.

He et al. [31] have performed voltammetric measurements to analyze how the solvent affects the Li-S redox chemistry for the present system. They considered nine solvents in a wide range of dielectric constants, including dimethyl sulfoxide (DMSO), dimethylformamide (DMF), dimethylacetamide (DMA), 1,2-dimethoxyethane (DME), tetraethylene glycol dimethyl ether (TEGDME), acetonitrile (ACN), sulfolane(TMS), 1,3-dioxolane:DME (DOL:DME) and 1,4-dioxane:DME(Diox:DME). The cathode consisted of a S_8/C composite. The voltammetric behaviour exhibited a considerable complexity, which the authors classified in a first approximation into two groups, depending on the number of oxidation and reduction peaks, and the peak separation of the reduction peaks. Generally speaking, the voltammetric behaviour of this system may exhibit up to three oxidation peaks and two reduction peaks. A deeper analysis by these authors resulted in a classification into three groups, depending on the rate of anodic/cathodic peaks: 3/2, 1/2, 1/1. In the case of the more negative couple of peaks, a straightforward correlation was found between its reversibility and the donor number of the solvent. This fact was explained in terms of the stabilization of different types of polysulfides, which exhibit different charge densities. In the case of the more positive reduction peak, there is consensus that this is due to the electrochemical reduction of S_8, So, we are only left with the *most positive oxidation peak* to try to draw some conclusions and correlate with the present calculations. This oxidation peak, which is found in the range 2.2-2.6 V vs Li/Li^+ , has a complex structure, is present even in quasi-solid-state S-Li systems and has been assigned to the oxidation of lithium sulfide to Li polysulfides/sulfur [44]. We will in the following, make an analysis of some properties of this peak from the data of He et al. [31]. While a correlation with the present calculations may be considered speculative, it is worth making this exercise, since we are convinced this will stimulate research in the present directions. For example, the same analysis may be performed with the donor number of the solvent; we will address this approach in the future. For the discussion, we will consider two characteristics of this oxidation peak, namely, its potential and its current density. Figure 8 shows the peak potential as a function of the inverse dielectric constant, and Figure 9 shows the corresponding plot for the peak current density. Although the points scatter heavily on these plots, two trends become apparent: On one side, the peak potential shifts towards more negative values (reaction becomes more reversible) as ε increases. On the other side, the peak current decreases as ε increases. At first sight, these two trends appear to be contradictory: how can a more reversible reaction (lower overpotential) present a reduced rate (lower current density? We will attempt an answer to this question in terms of the present modelling, although we acknowledge that more research is needed to reach a definite conclusion.

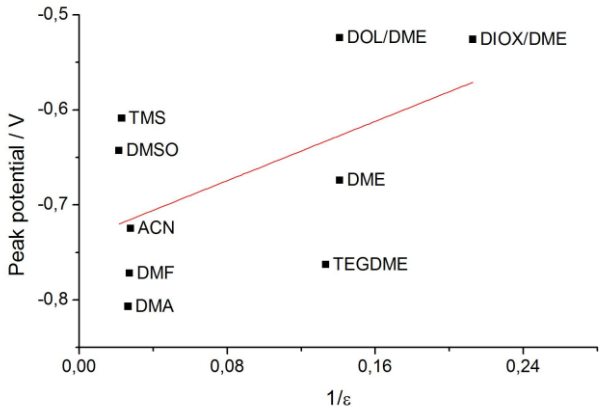

Figure 8. Peak potential for the most positive voltammetric oxidation peak observed on a glassy carbon electrode under an argon atmosphere at room temperature in various organic solvents with dissolved S_8, as a function of the inverse dielectric constant. Data were taken from reference [31]

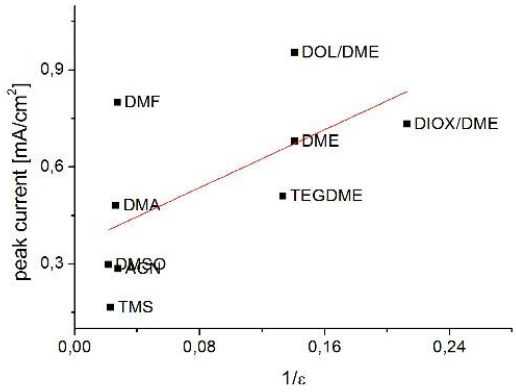

Figure 9: Peak current density for the most positive voltammetric oxidation peak, observed on a glassy carbon electrode under an argon atmosphere at room temperature in various organic solvents with dissolved S_8 , as a function of the inverse dielectric constant. Data were taken from reference [31]

To understand this apparent paradox, let us think of the Li_2S oxidation reaction as a first-order reaction, and let us write its decomposition as:

$$-\frac{d[Li_2S]}{dt} = K[Li_2S] \qquad \text{eq. (3)}$$

where $[Li_2S]$ represents the concentration of Li_2S molecules undergoing the reaction, adsorbed on the electrocatalyst and K is a rate constant, which in principle depends on the electrode potential. Following absolute rate theory, the rate constant K will be given by:

$$K = \frac{kT}{h} e^{-\frac{\Delta G^{\#}}{kT}} \qquad \text{eq. (4)}$$

where the preexponential factor contains the temperature and the Boltzmann and Planck constants, and $\Delta G^{\#}$ is the free energy of activation. The proper calculation of $\Delta G^{\#}$ and its dependence on electrode potential requires more developed modelling that the one we are presenting here, see for example the work of Ignazsak et al. [45] applied to the ORR. However, we keep the present discussion qualitative, and we lead it in terms of the contributions to equations (3) and (4) that can be inferred from the present modelling. In this context, two elements are essential in these equations. On one side the surface concentration $[Li_2S]$ and on the other side the free energy of activation $\Delta G^{\#}$. Concerning $[Li_2S]$, we conclude from the results of Figure 1, that an increasing dielectric constant will result in a decrease of $[Li_2S]$. This is so because a larger ε will produce a weaker attachment of Li_2S molecules to the surface, with the consequent decrease of $[Li_2S]$. This effect may be responsible for the decrease in the current density with increasing ε , shown in Figure 9. On the other hand, the activation $\Delta G\#$ may be decreased by an increasing ε, such as shown in Figure 4 for a graphene surface. This effect may explain the decrease of the peak potential with increasing ε, as shown above in Figure 8. Thus, the present modeling may deliver an explanation to the seemingly contradictory results presented in Figures 8 and 9. These are of course conclusions within the present simple modeling, since other elements, like the effect of the solvent donor number, should be taken into account.

4. Conclusions

We have taken first the steps to introduce in DFT calculations the effect of the dielectric constant of the solvent on the activation energy of the cleavage reaction of Li_2S on different catalytic surfaces. Two types of surfaces were considered, that present different interactions with the solvent: on one side graphene, that presents a weak interaction with a polarizable media, and on the other side two types of sulfides, that present a stronger interaction.

In both cases, the dielectric representing the solvent weakens the interaction of the molecule with the surface, but in the second case, the effect is considerably stronger, preventing the adsorption of the molecule for a large enough value.

Then the dissociation of the molecule was considered on the two types of surfaces. In all cases, the dielectric favours the breakage of the molecule, decreasing the activation energy for this process.

These theoretical findings were discussed in connection with experimental results from the literature, where the behavior of the Li-S cathode was studied in different solvents. According to this, the lower polarization observed for the electrooxidation of Li_2S in solvents with high dielectric constants could be related to the lower activation energy required for this process. On the other hand, a high dielectric constant delivers a lower concentration of the reacting molecules.

Acknowledgements

E.P.M. Leiva acknowledges grants PIP CONICET 11220150100624CO, PUE/2017 CONICET, FONCYT PICT-2015-1605 and SECyT of the Universidad Nacional de Córdoba. Support by CCAD-UNC and GPGPU Computing Group, Y-TEC and an IPAC grant from SNCAD-MinCyT, Argentina, are also gratefully acknowledged.

References

[1] Kim Y-R, Bong S, Kang Y-J, Yang Y, Mahajan R K, Kim J S and Kim H 2010 Electrochemical detection of dopamine in the presence of ascorbic acid using graphene modified electrodes. *Biosens. Bioelectron.* **25** 2366–9

[2] Zhang Z W, Peng H J, Zhao M and Huang J Q 2018 Heterogeneous/Homogeneous Mediators for High-Energy-Density Lithium–Sulfur Batteries: Progress and Prospects *Adv. Funct. Mater.* **28**

[3] Wang Y, Sahadeo E, Rubloff G, Lin C F and Lee S B 2019 High-capacity lithium sulfur battery and beyond: a review of metal anode protection layers and perspective of solid-state electrolytes *J. Mater. Sci.* **54** 3671–93

[4] Chen X, Hou T, Persson K A and Zhang Q 2019 Combining theory and experiment in lithium–sulfur batteries: Current progress and future perspectives *Mater. Today* **22** 142–58

[5] Zhang X Q, Liu C, Gao Y, Zhang J M and Wang Y Q 2020 Research Progress of Sulfur/Carbon Composite Cathode Materials and the Corresponding Safe Electrolytes for Advanced Li-S Batteries *Nano* **15** 1–13

[6] Fan X, Sun W, Meng F, Xing A and Liu J 2017 Advanced chemical strategies for lithium-sulfur batteries: A review *Green Energy Environ.* **3** 2–19

[7] Fan L, Deng N, Yan J, Li Z, Kang W and Cheng B 2019 The recent research status quo and the prospect of electrolytes for lithium sulfur batteries *Chem. Eng. J.* **369** 874–97

[8] Son Y, Lee J S, Son Y, Jang J H and Cho J 2015 Recent Advances in Lithium Sulfide Cathode Materials and Their Use in Lithium Sulfur Batteries *Adv. Energy Mater.* **5** 1–14

[9] Li S, Leng D, Li W, Qie L, Dong Z, Cheng Z and Fan Z 2020 Recent progress in developing Li2S cathodes for Li–S batteries *Energy Storage Mater.* **27** 279–96

[10] Su D, Zhou D, Wang C and Wang G 2018 Toward High Performance Lithium–Sulfur Batteries Based on Li2S Cathodes and Beyond: Status, Challenges, and Perspectives *Adv. Funct. Mater.* **28** 1–23

[11] Ye H, Li M, Liu T, Li Y and Lu J 2020 Activating Li2S as the Lithium-Containing Cathode in Lithium-Sulfur Batteries *ACS Energy Lett.* **5** 2234–45

[12] Wu F, Pollard T P, Zhao E, Xiao Y, Olguin M, Borodin O and Yushin G 2018 Layered LiTiO2 for the protection of Li2S cathodes against dissolution: Mechanisms of the remarkable performance boost *Energy Environ. Sci.* **11** 807–17

[13] Yuan H, Chen X, Zhou G, Zhang W, Luo J, Huang H, Gan Y, Liang C, Xia Y, Zhang J, Wang J and Tao X 2017 Efficient Activation of Li2S by Transition Metal Phosphides Nanoparticles for Highly Stable Lithium-Sulfur Batteries *ACS Energy Lett.* **2** 1711–9

[14] Liang X, Yun J, Xu K, Xiang H, Wang Y, Sun Y and Yu Y 2019 A multi-layered Ti3C2/Li2S composite as cathode material for advanced lithium-sulfur batteries *J. Energy Chem.* **39** 176–81

[15] Shin W, Lu J and Ji X 2019 ZnS coating of cathode facilitates lean-electrolyte Li-S batteries *Carbon Energy* **1** 165–72

[16] Guangmin Zhou, Hongzhen Tian, Yang Jin, Xinyong Tao, Bofei Liu, Rufan Zhang, Zhi Wei Seh, Denys Zhuo, Yayuan Liu, Jie Sun, Jie Zhao, Chenxi Zu, David Sichen Wu, Qianfan Zhang and Y Cui 2017 Catalytic oxidation of Li2S on the surface of metal sulfides for Li−S batteries PNAS 114 840–5

[17] He J, Chen Y and Manthiram A 2019 Metal Sulfide-Decorated Carbon Sponge as a Highly Efficient Electrocatalyst and Absorbant for Polysulfide in High-Loading Li2S Batteries *Adv. Energy Mater.* **9**

[18] Du G Y, Liu C Y and Li E Y 2020 A DFT investigation on the origins of solvent-dependent polysulfide reduction mechanism in rechargeable Li-s batteries *Catalysts* **10** 34–6

[19] Yang Y, Zheng G, Misra S, Nelson J, Toney M F and Cui Y 2012 High-capacity micrometer-sized Li 2S particles as cathode materials for advanced rechargeable lithium-ion batteries *J. Am. Chem. Soc.* **134** 15387–94

[20] Perdew J P, Burke K and Ernzerhof M 1996 Gga-Pbe *Phys. Rev. Lett.* **77** 3865–8

[21] STEFAN GRIMME 2006 Semiempirical GGA-Type Density Functional Constructed with a Long-Range Dispersion Correction *J. Comput. Chem.* **27** 1787–1799

[22] Hendrik J. Monkhorst and James D. Pack 1976 Special points for Brillonin-zone integrations *Phys. Rev. B 13, 5188* **13** 5188–92

[23] Henkelman G, Uberuaga B P and Jónsson H 2000 Climbing image nudged elastic band method for finding saddle points and minimum energy paths *J. Chem. Phys.* **113** 9901–4

[24] Lee S-K, Lee Y J and Sun Y-K 2016 Nanostructured lithium sulfide materials for lithium-sulfur batteries *J. Power Sources* **323** 174–88

[25] Eftekhari A and Kim D W 2017 Cathode materials for lithium-sulfur batteries: A practical perspective *J. Mater. Chem. A* **5** 17734–76

[26] Zhou G, Tian H, Jin Y, Tao X, Liu B, Zhang R, Seh Z W, Zhuo D, Liu Y, Sun J, Zhao J, Zu C, Wu D S, Zhang Q and Cui Y 2017 Catalytic oxidation of Li2S on the surface of metal sulfides for Li-S batteries *Proc. Natl. Acad. Sci. U. S. A.* **114** 840–5

[27] Kim S, Kim K, Park J and Sung Y 2019 Role and Potential of Metal Sulfide Catalysts in Lithium-Sulfur Battery Applications 2373–87

[28] Du G, Liu C and Elise Y. Li 2020 A DFT Investigation on the Origins of Solvent-Dependent Polysulfide Reduction Mechanism in Rechargeable Li-S BatteriesSolvent-Dependent Polysulfide Reduction *Catalysts* **10** 34–6

[29] Li Z, Zhou Y, Wang Y and Lu Y C 2019 Solvent-Mediated Li2S Electrodeposition: A Critical Manipulator in Lithium–Sulfur Batteries *Adv. Energy Mater.* **9** 1802207–17

[30] Zhejun Li, Haoran Jiang, Nien-Chu Lai, Tianshou Zhao and Y-C L 2019 Designing Effective Solvent−Catalyst Interface for Catalytic Sulfur Conversion in Lithium−Sulfur Batteries Chem. Mater 31 10186–96

[31] He Q, Gorlin Y, Patel M U M, Gasteiger H A and Lu Y-C 2018 Unraveling the Correlation between Solvent Properties and Sulfur Redox Behavior in Lithium-Sulfur Batteries *J. Electrochem. Soc.* **165** A4027–33

[32] Chu H, Jung J, Noh H, Yuk S, Lee J, Lee J, Baek J, Roh Y, Kwon H, Choi D, Sohn K, Kim Y and Kim H 2020 Unraveling the Dual Functionality of High-Donor-Number Anion in Lean-Electrolyte Lithium-Sulfur Batteries **2000493** 1–11

[33] Giannozzi P, Andreussi O, Brumme T, Bunau O, Nardelli M B, Calandra M, Car R, Cavazzoni C, Ceresoli D, Cococcioni M and others 2017 Advanced capabilities for materials modelling with Quantum ESPRESSO. (arXiv:1709.10010v1 [cond-mat.mtrl-sci]) *J. Phys. Condens. Matter* **29** 465901

[34] Andreussi O, Dabo I and Marzari N 2012 Revised self-consistent continuum solvation in electronic-structure calculations *J. Chem. Phys.* **136**

[35] Andreussi O, Georg N, Nattino F, Fisicaro G, Goedecker S and Marzari N 2019 Solvent-Aware Interfaces in Continuum Solvation *J. Chem. Theory Comput.* **15** 1996−2009

[36] Andreussi O and Marzari N 2014 Electrostatics of solvated systems in periodic boundary conditions *Phys. Rev. B - Condens. Matter Mater. Phys.* **90** 1–18

[37] A. Bondi 1964 van der Waals Volumes and Radii *J. Phys. Chem.* **68** 441–451

[38] Kavcı O and Cabuk S 2014 First-principles study of structural stability , elastic and dynamical properties of MnS *Comput. Mater. Sci.* **95** 99–105

[39] Wang W, Sun Z, Zhang W, Fan Q, Sun Q, Cui X and Xiang B 2016 First-principles investigations of vanadium disulfide for lithium and sodium ion battery applications *RSC Adv.* **6** 54874–9

[40] Ji Z, Contreras-torres F F, Jalbout A F and Ramírez-trevi A 2013 Surface diffusion and coverage effect of Li atom on graphene as studied by several density functional theory methods *Appl. Surf. Sci.* **285P** 846–52

[41] Li J, Qu Y, Chen C, Zhang X and Shao M 2021 Theoretical investigation on lithium polysulfide adsorption and conversion for high-performance Li–S batteries *Nanoscale* **13** 15–35

[42] Sun K, Wu Q, Tong X and Gan H 2018 Electrolyte with Low Polysulfide Solubility for Li-S Batteries *ACS Appl. Energy Mater.* **1** 2608–18

[43] Zhou G, Zhao S, Wang T, Yang S Z, Johannessen B, Chen H, Liu C, Ye Y, Wu Y, Peng Y, Liu C, Jiang S P, Zhang Q and Cui Y 2020 Theoretical Calculation Guided Design of Single-Atom Catalysts toward Fast Kinetic and Long-Life Li-S Batteries *Nano Lett.* **20** 1252–61

[44] Huang X, Wang Z, Knibbe R, Luo B, Ahad S A, Sun D and Wang L 2019 Cyclic Voltammetry in Lithium–Sulfur Batteries—Challenges and Opportunities *Energy Technol.* **7** 1–13

[45] Ignaczak A, Nazmutdinov R, Goduljan A, de Campos Pinto L M, Juarez F, Quaino P, Belletti G, Santos E and Schmickler W 2017 Oxygen Reduction in Alkaline Media—a Discussion *Electrocatalysis* **8** 554–64